An SEM examination of the chalcopyrite disease texture and its genetic implications

TOSHIRO NAGASE AND SHOJI KOJIMA

Institute of Mineralogy, Petrology and Economic Geology, Faculty of Science, Tohoku University, Aoba Sendai 980-77, Japan

Abstract

Back-scattered electron imaging with a scanning electron microscope was applied to the intimate association of fine chalcopyrite grains and sphalerite ('chalcopyrite disease') in synthesized products and natural specimens, in order to distinguish between diagnostic features of two formation mechanisms: replacement and coprecipitation. In the synthetic chalcopyrite disease in Fe-bearing sphalerite formed by a replacement reaction, chalcopyrite occurs as fine lamellae, which are also observed in relatively Fe-rich growth bands of the natural zoned sphalerite. Ellipsoidal to lens-like habits of chalcopyrite appear in sphalerite that has undergone extensive replacement reactions. These textures may have grown steadily from the lamellar chalcopyrite by consuming the FeS component dissolved in the sphalerite. All the sphalerite samples formed by the coprecipitation mechanism are Fe-poor, hosting triangular or irregularly bleb-like inclusions of chalcopyrite. This variety of chalcopyrite morphology could be attributed to diffusion rates and variations in fluid saturation, and their effect on the rate of crystal growth. Thus, in both replacement and coprecipitation the chalcopyrite habit depends strongly both on the FeS content of the host sphalerite and on kinetic factors, and is significant when interpreting chalcopyrite disease textures in natural samples.

KEYWORDS: back-scattered electron image, chalcopyrite disease, sphalerite, replacement reaction, coprecipitation mechanism, lamellae, triangular habit.

Introduction

THE intimate association of fine chalcopyrite and sphalerite, termed 'chalcopyrite disease' (Barton, 1978; Barton and Bethke, 1987) is characterized by the micrometre- to submicrometre-sized dusting and high density of chalcopyrite in sphalerite. Detailed discussions on the bulk composition of 'diseased' sphalerite (Sugaki *et al.*, 1987; Barton and Bethke, 1987; Shimazaki, 1988) have led most mineralogists to doubt the conventional idea of the involvement of an exsolution process, although exsolution clearly is important in sulphide ores formed at relatively high temperatures, such as metamorphosed ores. Recent hydrothermal experiments have clearly shown that the texture could result from either replacement (Kojima and Sugaki, 1987; Eldridge *et al.*, 1988) or coprecipitation (Kojima, 1990; Kojima *et al.*, 1995). In the case of replacement, it has been well documented that the chalcopyrite disease is formed by a reaction of Cu-bearing fluid with the FeS component dissolved in the sphalerite. Although Kojima (1990, 1992) refers to characteristics that might discriminate between the two formation mechanisms, many problems still remain.

Back-scattered electron (BSE) imaging with a scanning electron microscope (SEM) is a useful technique for characterizing mineral textures (e.g. Hall and Lloyd, 1981). This method gives not only a higher resolution of microscopic textures than that obtained by optical microscopy, but also gives an image brightness reflecting compositional variations. Thus BSE imaging is a most valuable technique to illustrate the textural features that result from replacement and coprecipitation, so that we may possibly devise criteria to distinguish between the two alternatives. In this paper, we compare textural features of chalcopyrite and sphalerite found in

Mineralogical Magazine, Vol. 61, February 1997, pp. 89–97

natural ores with experimentally synthesized samples (Kojima and Sugaki, 1987; Kojima, 1990), using BSE imaging and optical examination in transmitted light.

Analytical method and samples

BSE observations were carried out using a JEOL JSM-T330A equipped with a single p-n Si detector at 20 kV accelerating voltage. All samples were well polished and carbon-coated for SEM observation. The following six specimens were observed:

(a) The samples of Kojima and Sugaki (1987) synthesized experimentally by a process of replacement involving a reaction of natural sphalerite (Shinyemi mine, Korea) with Cu-bearing hydrothermal solutions at 400°C (sample nos. 4R12, 4R28).

(b) The sample of Kojima (1990) synthesized hydrothermally by a process of coprecipitation at 300°C (sample no. SC02).

(c) Natural samples from the Toyoha, the Furutobe and the Ezuri mines, Japan.

The Toyoha mine, situated in western Hokkaido, is classified as a typical polymetallic epithermal vein-type (e.g. Kanbara *et al.*, 1989; Ohta, 1989), and the sphalerite ore from the Izumo vein was used for this study. The Furutobe and Ezuri deposits are located in Akita Prefecture and belong to the Kuroko-type; the former is the mine where chalcopyrite disease was first discussed by Barton (1978). For the studied samples, the associated minerals, the lattice parameter of the host sphalerite and the bulk composition of the diseased sphalerite were previously examined and are summarized in Table 1. The lattice parameter and bulk composition were determined by Guinier-Hägg camera method and electron-microprobe analysis using energy dispersive spectrometry, respectively. In the latter analysis, bulk compositions were measured with a wide beam ($\sim$20 μm) in the manner described by Sugaki *et al.* (1987). The minor elements normally included in sphalerite, such as Mn, Cd and In are not shown in Table 1, since they were in very low concentration in most of the natural specimens analysed. However, In contents in the Toyoha sample are appreciable, ranging up to $\sim$1.0 mol.% InS.

The brightness of a BSE image depends on the formula weight of the observed phase (atomic-number contrast: Hall and Lloyd, 1981). The relative brightness of the phases of interest in this study should increase in the order of chalcopyrite ($CuFeS_2$), Fe-rich sphalerite ($Zn_{0.8}Fe_{0.2}S$) and sphalerite (ZnS), based on the trend in respective formula weight: 92.7, 95.5, and 97.5. Characteristic features of the chalcopyrite disease textures in the six samples are described below, divided into the two groups: synthetic products and natural specimens.

Results

Synthesized products

Replacement texture. The periphery of the experimentally reacted sphalerite (Kojima and Sugaki, 1987) is substituted by newly formed chalcopyrite and many tiny cracks cut across both minerals. In the 4R12 sample, lamellar chalcopyrite crystals (<5 μm) are visible (Fig. 1*a*). The image contrast between chalcopyrite and sphalerite is not distinct, because the sphalerite in this sample is Fe-rich (see Table 1). In the highly reacted sample (4R28), many small pores resulting from hydrothermal reactions are observed in the periphery of the sphalerite (the dark spots in Fig. 1*b*). Such porous areas show brighter images than the central part of the sphalerite (Fig. 1*b*), suggesting that considerable reduction of Fe occurs at the sphalerite adjacent to chalcopyrite. The chalcopyrite replacing the periphery of the sphalerite and the host sphalerite contain small inclusions of nearly pure sphalerite (the white spots in Fig. 1*b*, *c*), which are regarded as products recrystallized by hydrothermal reactions (Kojima and Sugaki, 1987). These recrystallized sphalerite crystals are almost always associated with pores in the chalcopyrite and host sphalerite (see Fig. 1*b*, *c*). As shown in the magnified image of Fig. 1*b* (Fig. 1*c*), slightly lighter halos suggestive of a local heterogeneity in Fe content develop in contact with both pores and chalcopyrite grains in the sphalerite. In contrast to the lamellar chalcopyrite in 4R12, some chalcopyrite in 4R28 appears to have coarser habits, such as ellipsoidal and lens-like.

Coprecipitation texture. The experimental product (SC02) synthesized by Kojima (1990) shows a typical association of sphalerite and micrometre-sized chalcopyrite inclusions, and the FeS content of the host sphalerite is regarded as being uniformly low (see Table 1). Accordingly, clear image contrasts were obtained in this sample (Fig. 2). The inclusions of chalcopyrite are micromtre- and submicrometre-sized, frequently showing triangular habits (Fig. 2*b*), and no cubic forms of chalcopyrite were found; the three dimensional shape of these inclusions is tetrahedral. Figure 2*b* suggests that the triangular inclusions of chalcopyrite are orientated topotaxially with respect to the host sphalerite. In this sample, irregularly polyhedral inclusions of chalcopyrite with a grain size up to 5 μm are also observed (Fig. 2*a*).

Natural samples

Toyoha mine. A marked compositional zonation of FeS in sphalerite and several chalcopyrite veinlets cutting across the zoned sphalerite are clearly observed in the sphalerite-rich ore from this deposit.

TABLE 1. A summary of lattice parameters and compositional ranges of the sphalerite samples and associated minerals

Sample	Colour	Shape of chalcopyrite	Associated minerals	Lattice parameter (Å)	Compositional range (mol.%)* CuS	FeS	ZnS	
Synthetic** (4R12, 4R28)	red brown ~ orange	lamellar lens-like	pyrite, bornite	5.4217(4)	4.7–9.7	12.4–15.8	76.8–79.2	[1]
Synthetic (SC02)	colourless	triangular polyhedral	pyrite, bornite, covellite	5.4099(6)	1.3–3.3	1.4–3.3	93.5–97.0	[2]
Toyoha**	red brown ~ orange	lamellar	pyrite, galena roquesite	5.4159(5)	3.5–9.0	6.8–10.9	80.7–88.0	
Furutobe	colourless ~ light yellow	bleb-like lamellar	galena, pyrite tetrahedrite, (hematite)	5.4094(5)	~ 3.0	3.2–3.4	93.6–93.8	[3]
Ezuri	colourless	bleb-like	pyrite, galena, tetrahedrite, bornite	5.4111(3)	0.7–2.9	0.3–2.8	93.4–97.9	

* Bulk compositions of diseased sphalerite.
** Diseased zone shows significant anisotropy.
[1] Kojima and Sugaki (1987); [2] Kojima (1990); [3] Sugaki *et al.* (1987).

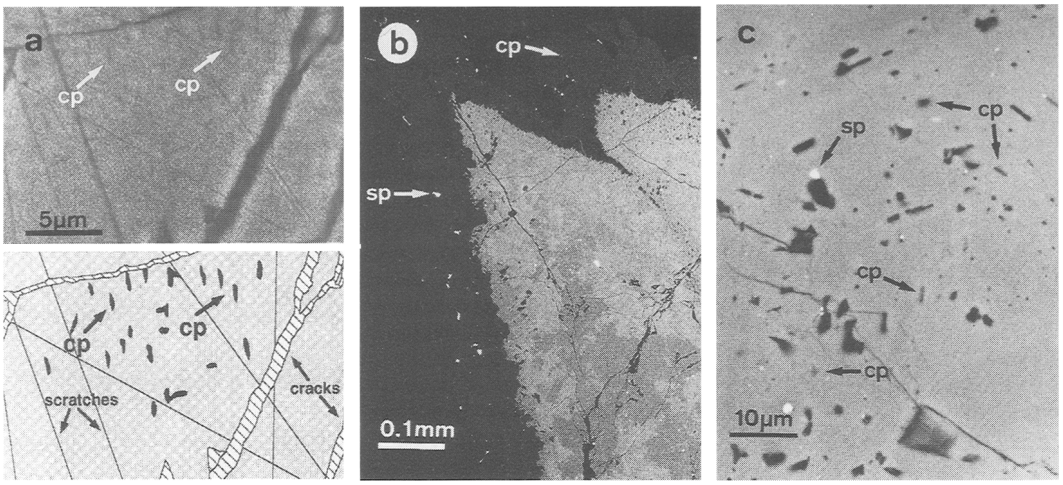

FIG. 1. Back-scattered electron images of the replacement products synthesized by Kojima and Sugaki (1987). (*a*) Sample 4R12. Many chalcopyrite lamellae occur near cracks in sphalerite (dark gray); (*b*) Sample 4R28. Hydrothermally reacted sphalerite, whose periphery is substituted by chalcopyrite (dark gray). Black and white spots are pores and recrystallized sphalerite with the nearly pure composition, respectively. The periphery of sphalerite shows a considerable reduction of Fe (lighter part); (*c*) Sample 4R28. Magnified image of (*b*) showing ellipsoidal to lens-like habits of chalcopyrite inclusions. Except for the irregularly-shaped pores along the cracks, the dark spots represent chalcopyrite grains. Abbreviations: cp, chalcopyrite; sp, sphalerite. See text for detailed explanations.

(Fig. 3*a*). The Fe-zonation has no textural conformity with the chalcopyrite veinlets and is therefore a primary feature. As described earlier, the sphalerite sample contains appreciable amounts of In, and so the image contrast of the zonal structure is enhanced. Bleb-like chalcopyrite crystals (<10 μm) are typically observed in small cracks within the zoned sphalerite (Fig. 3*b*). Figure 3*c* shows that lamellar chalcopyrite crystals (<10 μm), as observed in Fig. 1*a*, occur within the zoned sphalerite which is of relatively Fe-poor composition in contrast to the chalcopyrite-free sphalerite without the distinct zonations. Furthermore, although the lamellae appear to be distributed homogeneously in the zoned sphalerite, the more

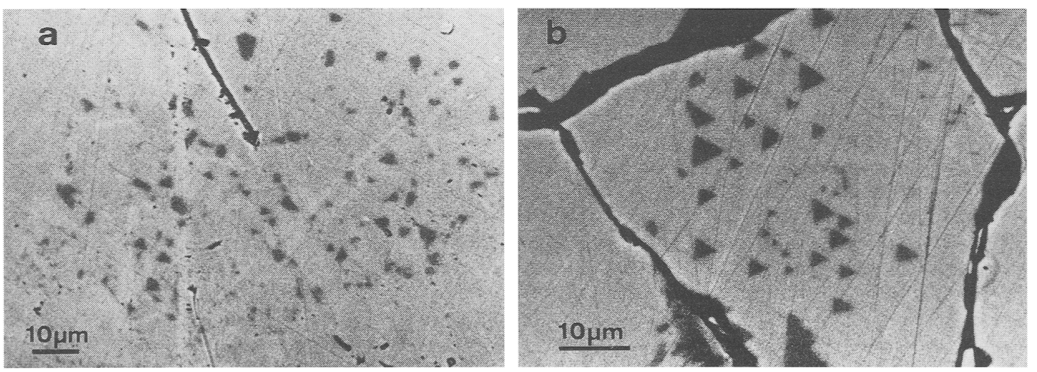

FIG. 2. Back-scattered electron images of the coprecipitation product (SC02) synthesized by Kojima (1990). (*a*) Irregularly polyhedral inclusions of chalcopyrite in sphalerite; (*b*) Triangular chalcopyrite crystals oriented topotaxially with respect to host sphalerite. See text for detailed explanations.

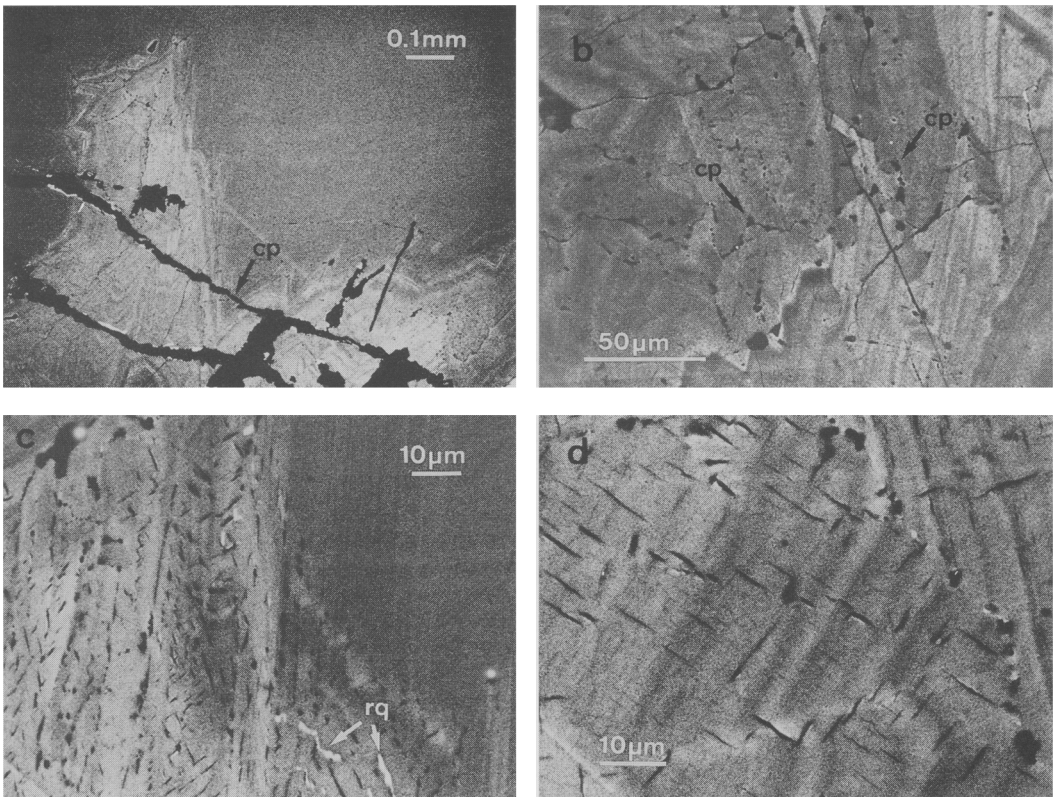

FIG. 3. Back-scattered electron images of the Toyoha sample. (*a*) Growth bands in sphalerite cut by chalcopyrite veinlet (dark black); (*b*) Bleb-like crystals of chalcopyrite occurring in cracks within zoned sphalerite; (*c*) Many lamellae of chalcopyrite in zoned sphalerite; (*d*) Magnified image of (*c*) showing lamellar chalcopyrite crystals developing along perpendicular crystallographic directions in sphalerite. Abbreviations: cp, chalcopyrite; rq, roquesite. See text for detailed explanations.

magnified image (Fig. 3*d*) shows that the chalcopyrite lamellae are mostly associated with relatively Fe-rich microbands and that most of them are in parallel or perpendicular relation to the growth bands. The diseased area shows distinct anomalous anisotropy under cross-polarized, reflected light.

Furutobe mine. The studied sample is identical to that examined by Sugaki *et al.* (1987) and is poor in FeS (see Table 1). Chalcopyrite and sphalerite are therefore imaged clearly because of the atomic-number contrast. In this sample, both lamellar and bleb-like habits are observed (Fig. 4*a*, *b*). In contrast to the sample from the Toyoha mine, however, chalcopyrite lamellae are larger ($\sim$10 μm), having a distribution limited to the area depleted in bleb-like chalcopyrite inclusions. Most lamellae in the periphery of the sphalerite are in two perpendicular orientations (Fig. 4*b*). In general, the grain size of the chalcopyrite inclusions in the periphery is smaller than that at the central part of the sphalerite. As shown in Table 1, the sphalerite sample is nearly colourless to light yellow in transmitted light, and growth bands, as found in the Toyoha sample, are not observed.

Ezuri mine. The image contrast between chalcopyrite and sphalerite for the sample from this deposit is distinct because the FeS content of sphalerite in this sample is very low (see Table 1). Chalcopyrite inclusions that vary in size up to 10 μm are randomly distributed in the sphalerite and some of the granular inclusions exhibit planar relationships (Fig. 4*c*). The inclusions show a tendency to be smaller in areas that are rich in inclusions. As shown in Fig. 4*d*, the chalcopyrite inclusions exhibit irregularly bleb-like habits. The lamellar habit of chalcopyrite is not observed in the sphalerite, and thus morphological variety is limited as compared with the Furutobe sample. The host sphalerite is almost colourless

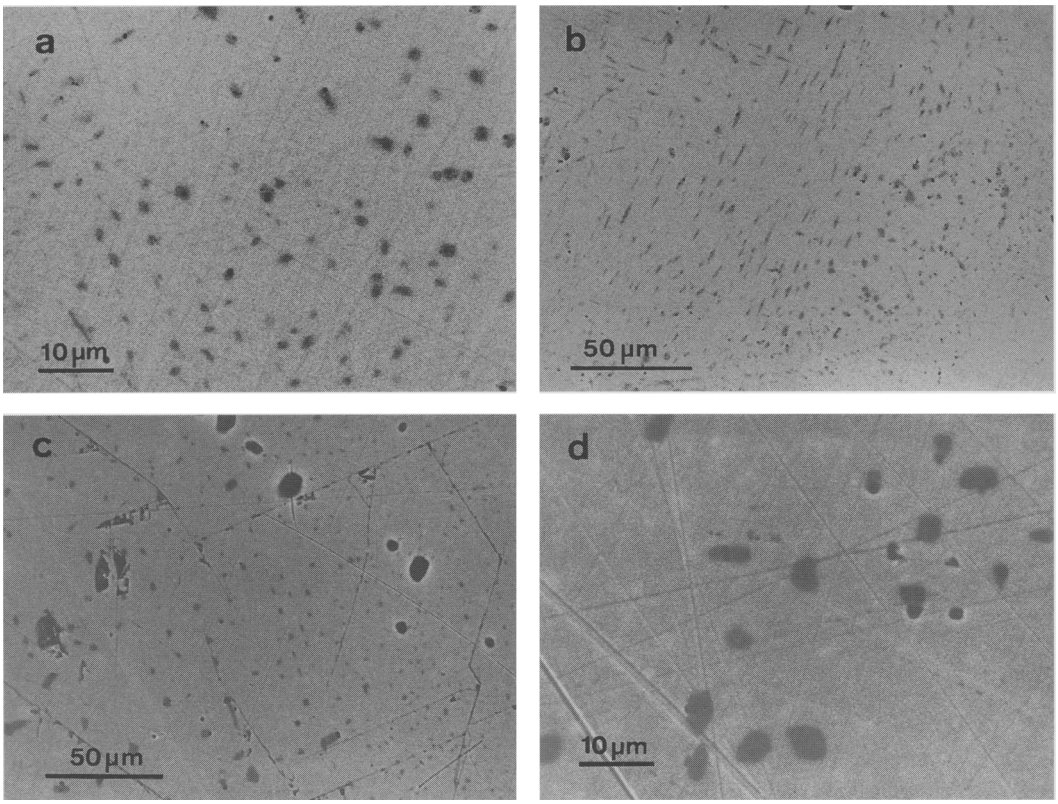

FIG. 4. Back-scattered electron images of the samples from the Furutobe (*a* and *b*) and Ezuri (*c* and *d*) deposits. (*a*) Bleb-like inclusions of chalcopyrite in sphalerite; (*b*) Lamellar inclusions of chalcopyrite coexisting with bleb-like ones in sphalerite; (*c*) Bleb-like inclusions of chalcopyrite in a fairly epitaxial relation to host sphalerite; (*d*) Magnified image of (*c*) showing bleb-like habits of chalcopyrite. See text for detailed explanations.

under transmitted light, having no growth bands as shown in Fig. 3. The distinct anomalous anisotropy observed in the Toyoha sample is not seen in the Furutobe and Ezuri samples.

Discussion

A comparison of textural features in natural specimens with those in synthesized products can lead to interpretation of the formation process of the chalcopyrite disease texture. Therefore, we will consider the chalcopyrite disease textures in the natural specimens in the light of those in the synthesized products.

Toyoha sample. The occurrence of lamellar chalcopyrite is common to the 4R12 and Toyoha samples, leading us to suggest that the chalcopyrite disease texture in the Toyoha sample is attributable to replacement. The Widmanstätten-like feature (Fig. 3*d*) is generally regarded as resulting from simple exsolution, but it is clear that replacement can also produce a lamellar habit of chalcopyrite in sphalerite. As described earlier, the diseased area of the Toyoha sphalerite along the chalcopyrite veinlets shows distinct anomalous anisotropy under crossed-polarized reflected light. We believe that this feature is also indicative of replacement reactions (Kojima, 1992), although Barton and Bethke (1987) have noted the opposite effect, that the diseased crystals are less anisotropic than original ones. The bulk Cu content of the Toyoha sphalerite (see Table 1) is far above the solubility limit of Cu in sphalerite solid-solution determined in the Cu-Fe-Zn-S system (<2.4 mol.% CuS at 300–500°C; Kojima and Sugaki, 1985), and so it is highly unlikely that the lamellar chalcopyrite was an exsolved product. Recently, Pattrick *et al.* (1993) have described submicrometre-sized chalcopyrite inclusions in an Fe-rich microband of the West Shropshire (England) sphalerite, which are regarded as locally diffusion-

controlled exsolution products. In the case of the Toyoha sample, however, we note that the existence of the growth bands with the chalcopyrite disease argues against wholesale diffusion that would have permitted exsolution (P.B. Barton, Jr., pers. commun.).

Furthermore, it has been frequently noted that the FeS content of primary sphalerite decreases by later reactions such as replacement and retrograde metamorphism (e.g. Kojima and Sugaki, 1987; Mariko, 1988; Toulmin *et al.*, 1991), but considerable increases of Fe in sphalerite undergoing replacement have not yet been documented (Kojima, 1992). These relations suggest that the host sphalerite must have originally contained a considerable amount of Fe to have been able to form the fine lamellae of chalcopyrite. In the highly replaced sample (4R28), ellipsoidal to lens-like habits of chalcopyrite were observed (Fig. 1*c*). This fact suggests that the lamellar chalcopyrite grows into the lens-like habit; indeed such a phenomenon has been recognized in the Kamioka (Japan) sphalerite of Mariko (1988). The unit-cell volume of sphalerite must be reduced when the FeS in sphalerite is consumed to form chalcopyrite (e.g. Barton and Bethke, 1987), and so the small cracks observed in the synthetic and Toyoha samples may have been induced by the volume reduction.

Kojima and Sugaki (1987) and Eldridge *et al.* (1988) have confirmed that fine lamellae of chalcopyrite are formed by a reaction of Cu-bearing fluid with FeS in sphalerite. However, a variety of mechanisms are proposed for the replacement reactions (see Kojima, 1990). For the Toyoha sample, we prefer a Cu-diffusion mechanism in sphalerite with enhancement by fluids because no features suggestive of extensive dissolution-reprecipitation of sphalerite were observed. Recent studies on metal diffusion in sphalerite (Nelkowski and Bollman, 1969; Goble *et al.*, 1979; Mizuta, 1988) have shown that the interdiffusion rate of Fe is very slow compared with that of Cu. Accordingly, the probability of chalcopyrite nucleation and its distribution are controlled mainly by the diffusivity of Cu. From a kinetic point of view, however, the growth of chalcopyrite inclusions should depend on the diffusivity of Fe in sphalerite. Therefore, the diffusion rate of Fe in sphalerite would provide a constraint on the time needed for the chalcopyrite-formation in the case of replacement reactions. An estimate using the diffusion coefficient of Fe in Fe-rich sphalerite by Mizuta (1988) and assuming isothermal annealing shows that Fe in sphalerite can move a distance of $\sim$10 μm over only $\sim$780 years at 300°C (the approximate temperature of formation; Ohta, 1989) and over $\sim$640,000 years at 200°C. These values are within the absolute age for formation of the Toyoha deposit ($\sim$1.8 m.y.; Sawai *et al.*, 1989). These calculations are based on the assumption that transfer of the constituent elements is controlled by solid-state lattice diffusion. Nevertheless the result can well explain the spatial distribution of chalcopyrite inclusions in the Toyoha sphalerite. We can safely conclude that the chalcopyrite lamellae in the sample from the young Toyoha deposit is an incipient feature in the replacement.

Furutobe and Ezuri samples. In the case of the Furutobe sample, it is difficult to judge whether or not the lamellar chalcopyrite formed by a replacement reaction. The Furutobe sphalerite has a low FeS content (see Table 1), and the distribution of chalcopyrite lamellae in the sphalerite is restricted, in contrast to the Toyoha sample. Furthermore, the chalcopyrite lamellae appear to be epitaxially oriented in the host sphalerite. Thus it seems unlikely that the lamellar chalcopyrite in the Furutobe sphalerite results from replacement. Irregular bleb-like inclusions of chalcopyrite are very common in the sample from both the Furutobe and Ezuri mines (see Fig. 4*a*, *c*). Both samples are very similar to the synthesized product (SC02) in that such bleb-like inclusions of chalcopyrite are hosted in Fe-poor sphalerite. Therefore, we prefer an interpretation that many of the chalcopyrite inclusions in sphalerite from the Furutobe and Ezuri mines have been formed by the coprecipitation mechanism. The chalcopyrite inclusions in the Ezuri sphalerite are partially arranged in bands. This would represent the epitaxial nucleation of chalcopyrite at the growing surface of sphalerite. Some of the chalcopyrite grains found in the synthesized product tends to exhibit triangular shapes, in contrast to those in the two Kuroko-type deposits. Nevertheless, the triangular shape is also observed in some kinds of massive sulphide deposits, such as modern seafloor deposits (e.g. Okinawa Trough), Mississippi Valley-type deposits and Kuroko-type deposits (Kojima, 1990; P.B. Barton, Jr., pers. comm.). Thus, the triangular habit of chalcopyrite in sphalerite may be common to massive sulphide deposits formed under submarine conditions. It is difficult to judge whether the bleb-like shape is a kind of spherule or a dissolution feature of an originally triangular habit. In the former case, we suggest that the chalcopyrite inclusions in sphalerite from the Kuroko deposits were formed under a higher degree of supersaturation with respect to chalcopyrite than in the synthetic product showing the triangular habit.

Summary

A summary of all the properties in the synthetic and natural chalcopyrite disease textures is listed in

TABLE 2. A summary of various properties of the chalcopyrite disease texture as functions of processes

Mechanism	Process	Chalcopyrite habit	Remarks
Replacement	Chalcopyrite nucleation by a reaction of Cu-bearing fluid with FeS in sphalerite	lamellar	anisotropic (?) Fe-rich sphalerite
	Subsequent growth of chalcopyrite by consuming Fe in sphalerite	lens-like, ellipsoidal	
Coprecipitation	Rapid nucleation of chalcopyrite with overgrowth of sphalerite	triangular irregularly polyhedral	sector structure
	Epitaxial nucleation of chalcopyrite at growing front of sphalerite	bleb-like, blocky lamellar (?)	

Table 2. These data suggest that the processes of replacement and coprecipitation are characterized by the lamellar and triangular habits of chalcopyrite, respectively. The replacement mechanism occurs only in Fe-bearing sphalerite, and subsequently the lamellar chalcopyrite would grow into lens-like or ellipsoidal chalcopyrite at the expense of FeS dissolved in host sphalerite. We conclude that the habit of chalcopyrite found in chalcopyrite disease textures depends strongly on sphalerite composition (FeS content) and kinetic factors, and this feature should be helpful in interpreting chalcopyrite disease textures. As a next step, we need to examine the internal structure of 'diseased' sphalerite and interface coherency between chalcopyrite and host sphalerite for the samples. These results will be evaluated in the future using high-resolution transmission electron microscopy (HRTEM).

Acknowledgements

We wish to thank I.N. MacInnis, who improved an earlier manuscript and M. Akizuki for his useful suggestions. Also we thank H. Fujimaki, who kindly assisted in the EPMA analyses. We would like to thank P.B. Barton, Jr., P.E. Brown, and an anonymous reviewer for their fruitful and constructive discussions. The expense of this study was partially defrayed by a Grant-in-Aid for Scientific Research (No. 07740419) from the Ministry of Education, Science and Culture of Japan, to which we express our sincere thanks.

References

Barton, P.B., Jr. (1978) Some ore textures involving sphalerite from the Furutobe mine, Akita Prefecture, Japan. *Mining Geol.*, **28**, 293–300.

Barton, P.B., Jr. and Bethke, P.M. (1987) Chalcopyrite disease in sphalerite: pathology and epidemiology. *Amer. Mineral.*, **72**, 451–67.

Eldridge, C.S., Bourcier, W.L., Ohmoto, H. and Barnes, H.L. (1988) Hydrothermal inoculation and incubation of the chalcopyrite disease in sphalerite. *Econ. Geol.*, **83**, 978–89.

Goble, R.J., Scott, S.D. and Hancock, R.G.V. (1979) Diffusion rates of Zn and Fe in sphalerite (abst.). Geol. Assoc. Canada, Mineral. Assoc. Canada, and Canadian Soc. Petroleum Geol., Annual Meet. Program with Abstracts, 4, 53.

Hall, M.G. and Lloyd, G.E. (1981) The SEM examination of geological samples with a semiconductor back-scattered electron detector. *Amer. Mineral.*, **66**, 362–8.

Kanbara, H., Sanga, T., Ohura, T. and Kumita, K. (1989) Mineralization of Shinano vein in the Toyoha polymetallic vein-type deposits, Hokkaido, Japan. *Mining Geol.*, **39**, 107–22 (in Japanese).

Kojima, S. (1990) A coprecipitation experiment in intimate association of sphalerite and chalcopyrite and its bearings on the genesis of Kuroko ores. *Mining Geol.*, **40**, 147–58.

Kojima, S. (1992) The nature of chalcopyrite inclusions in sphalerite: exsolution, coprecipitation, or 'diseased'? - A discussion. *Econ. Geol.*, **87**, 1191–2.

Kojima, S. and Sugaki, A. (1985) Phase relations in the Cu-Fe-Zn-S system between 500° and 300°C under hydrothermal conditions. *Econ. Geol.*, **80**, 158–71.

Kojima, S. and Sugaki, A. (1987) An experimental study on chalcopyritization of sphalerite induced by hydrothermally metasomatic reactions. *Mining Geol.*, **37**, 373–80.

Kojima, S., Nagase, T. and Inoue, T. (1995) A coprecipitation experiment on the chalcopyrite disease texture involving Fe-bearing sphalerite. *J. Mineral. Petrol. Econ. Geol.*, **90**, 261–7.

Mariko, T. (1988) Compositional zoning and 'chalcopyrite disease' in sphalerite contained in the Pb-Zn-quartz-calcite ore from the Mozumi deposit of the Kamioka mine, Gifu Prefecture, Japan. *Mining*

Geol., **38**, 393–400 (in Japanese).

Mizuta, T. (1988) Interdiffusion rate of zinc and iron in natural sphalerite. *Econ. Geol.*, **83**, 1205–20.

Nelkowski, F.R.N. and Bollman, G. (1969) Diffusion von In und Cu in ZnS-einkristallen. *Zeitschr. Naturforsch.*, **24a**, 1302–6.

Ohta, E. (1989) Occurrence and chemistry of indium-containing minerals from the Toyoha mine, Hokkaido, Japan. *Mining Geol.*, **39**, 355–72.

Pattrick, R.A.D., Dorling, M. and Polya, D.A. (1993) TEM study of indium- and copper-bearing growth-banded sphalerite. *Can. Mineral.*, **31**, 105–17.

Sawai, O., Okada, T. and Itaya, T. (1989) K-Ar ages of sericite in hydrothermally altered rocks around the Toyoha deposits, Hokkaido, Japan. *Mining Geol.*, **39**, 191–204.

Shimazaki, H. (1988) On chalcopyrite disease texture. In: *Ore Microscope and Ore Textures* (A. Sugaki, ed.), Terra Scientific Publishing Company, Tokyo, 397–413 (in Japanese).

Sugaki, A., Kitakaze, A. and Kojima, S. (1987) Bulk compositions of intimate intergrowths of chalcopyrite and sphalerite and their genetic implications. *Mineral. Deposita*, **22**, 26–32.

Toulmin, P. III, Barton, P.B., Jr. and Wiggins, L.B. (1991) Commentary on the sphalerite geobarometer. *Amer. Mineral.*, **76**, 1038–51.

[*Manuscript received 11 August 1995: revised 7 June 1996*]